Ionic Conductivity of Potassium Phosphatoantimonates and Some of Their Ion-Exchanged Analogues

E. Wang and M. Greenblatt*

Department of Chemistry, Rutgers, The State University of New Jersey, Piscataway, New Jersey 08854

Received January 16, 1991. Revised Manuscript Received March 18, 1991

The ionic conductivity in quasi-one-dimensional (1D) K_2SbPO_6, quasi-two-dimensional (2D) $KSbP_2O_8$ and $K_3Sb_3P_2O_{14}$, and network-three-dimensional (3D) $K_5Sb_5P_2O_{20}$ and KSb_2PO_8 was studied. The dominant factor affecting the ionic conductivity, which is highest, $\sim 10^{-3}$ $(\Omega \cdot cm)^{-1}$, in $K_5Sb_5P_2O_{20}$ and lowest, $\sim 10^{-7}$ $(\Omega \cdot cm)^{-1}$, in KSb_2PO_8 at 500 °C, is the size of the bottleneck rather than the "dimensionality". The highest ionic conductivity observed in $K_5Sb_5P_2O_{20}$ was further improved in the ion-exchanged compound $Na_5Sb_5P_2O_{20}$ to $\sim 10^{-2}$ $(\Omega \cdot cm)^{-1}$ at 500 °C. Direct ion-exchange reactions with cations smaller than K^+ are not possible in 2D $KSbP_2O_8$ and 1D K_2SbPO_6. Rb_2SbPO_6 is a new compound synthesized via ion exchange from K_2SbPO_6. The ionic conductivity and ion-exchange behavior are discussed in terms of the structural properties of the potassium phosphatoantimonates.

Introduction

Recently Piffard et al. have synthesized a series of potassium phosphatoantimonates, K–O–Sb^v–P^v (henceforth abbreviated as KPA). The basic building units of these KPAs are SbO_6 octahedra and PO_4 tetrahedra. Depending on the arrangements of SbO_6 with PO_4, KPAs with "dimensionalities" ranging from "1D" in K_2SbPO_6,[1] "2D"in $KSbP_2O_8$[2] and $K_3Sb_3P_2O_{14}$,[3] to "3D" in $K_5Sb_5P_2O_{20}$[4] and KSb_2PO_8[5] have been synthesized (Figure 1). In K_2SbPO_6, edge-sharing SbO_6 octahedra corner share with PO_4 tetrahedra to form infinite chains along the *b* axis. The K^+ ions are located in tunnels formed between those chains. In the case of $KSbP_2O_8$ and $K_3Sb_3P_2O_{14}$, the structures can be best described as made up of infinite $(SbP_2O_8^-)$ and $(Sb_3P_2O_{14}^{3-})$ layers, respectively. Each layer is built up from corner-sharing SbO_6 octahedra and PO_4 tetrahedra with K^+ ions located between the layers. The interlayer distance is 8.47 Å for $KSbP_2O_8$ and 10.312 Å for $K_3Sb_3P_2O_{14}\cdot xH_2O$.

$K_5Sb_5P_2O_{20}$ and KSb_2PO_8 are framework structures in which SbO_6 octahedra share both corners and edges with one another and are also linked to the PO_4 tetrahedra via corners. However, $K_5Sb_5P_2O_{20}$ forms a skeleton structure (similar to the nasicon family) with large 3D interconnecting tunnels, whereas in KSb_2PO_8 the tunnel (smaller than that in $K_5Sb_5P_2O_{20}$) is only along the *b* axis. Moreover, in KSb_2PO_8 there is no unshared vertex of the PO_4 tetrahedron pointing into the layer or the tunnels as is the case in the other aforementioned KPAs.

These KPAs (except for K_2SbPO_6 and KSb_2PO_8) have been shown to possess good ion-exchange properties[6,7] and the $H_nSb_nP_2O_{3n+5}\cdot xH_2O$ (n = 1, 3, 5) analogues good proton conductivity.[8] It is the purpose of this paper to examine the ionic conductivities of the various KPAs in view of their structural differences and to improve (if possible) their ionic conductivity by replacing K^+ with other alkali-metal ions via ion exchange.

Experimental Section

All samples were prepared as reported by using KNO_3, Sb_2O_3, and $NH_4H_2PO_4$ as starting materials.[1-5] Exact molar ratios of the ingredients were mixed thoroughly in an agate mortar. Mixtures of $KSbP_2O_8$ and KSb_2PO_8 were heated at 200 °C to decompose ammonium monophosphate before final calcination at 920 °C. All other samples prepared were initially heated at 300 °C to decompose ammonium monophosphate before final calcination at 1000 °C.

Ion exchange was carried out to replace K^+ by other alkali-metal ions. Three different ion-exchange techniques were employed. In the molten salt technique, the KPAs were immersed in molten alkali nitrates ANO_3 (A = Li, Na, Rb, Cs) for about 4 h with a sample-to-salt weight ratio of 1:8. In the second technique, KPAs were mixed with slightly excess amounts of NaI and reacted in a vacuum-sealed quartz tube. Only NaI was tried as the ion-exchanging salt since both NaI and KI melt around the same temperature range, 660–680 °C. Finally, hydrothermal reaction in an autoclave was also used to exchange K^+ by other alkali-metal ions (A = Cs, Rb, Na, Li). Approximately 1 g of KPA sample was soaked in about 45 mL of 1 M aqueous alkali-metal nitrate solution. The reaction temperature varied from 150 to 200 °C, and the duration of reaction was about 12 h.

Samples were identified by using a Scintag PAD V automated powder diffractometer with monochromatized Cu Kα radiation. High-temperature X-ray powder diffraction was performed on a Scintag PAD V diffractometer equipped with a built-in furnace that was controlled with an Anton PAAR KG Model HTK 10 temperature controller. The sample was mounted on a platinum strip (that also acts as the heating element) and equilibrated at selected temperatures for about 10 min before it was analyzed by X-ray diffraction. Loss of water was monitored in a Du Pont 951 thermogravimetric analyzer (TGA). Ionic conductivity measurements were carried out by an ac complex impedance technique using a Solartron 1250 frequency analyzer and a 1186 electrochemical interface. Data collection and analysis were done on a Hewlett-Packard 9816 desktop computer. Samples were pelletized and sintered at 700 °C for a few hours before coating the surfaces of the pellets with platinum paste. A frequency range of 10 Hz to 65 kHz was employed at a heating rate of 3 °C/min from 200 to 650 °C in flowing helium. Measurements were carried out for each sample at least twice; the data are reproducible in each case. Chemical analysis was carried out with a Beckman plasma emission spectrometer.

Results

As was reported by Piffard et al.,[3] one of the KPAs was found to be hydrated at room temperature, which raises

(1) Lachgar, A.; Deniard-Courant, S.; Piffard, Y. *J. Solid State Chem.* **1986**, *63*, 409.
(2) Piffard, Y.; Oyetola, S.; Courant, S.; Lachgar, A. *J. Solid State Chem.* **1985**, *60*, 209.
(3) Piffard, Y.; Lachgar, A.; Tournoux, M. *J. Solid State Chem.* **1985**, *58*, 253.
(4) Piffard, Y.; Lachgar, A.; Tournoux, M. *Mater. Res. Bull.* **1986**, *21*, 1231.
(5) Piffard, Y.; Lachgar, A.; Tournoux, M. *Mater. Res. Bull.* **1985**, *20*, 715.
(6) Piffard, Y.; Verbaere, A.; Oyetola, S.; Deniard-Courant, S.; Tournoux, M. *Eur. J. Solid State Inorg. Chem.* **1989**, *26*, 113.
(7) Piffard, Y.; Verbaere, A.; Lachgar, A.; Deniard-Courant, S.; Tournoux, M. *Rev. Chim. Mineral.* **1986**, *23*, 766.
(8) Yoshikado, S.; Ohachi, T.; Taniguchi, I.; Onoda, Y.; Watanabe, M.; Fujiki, Y. *Solid State Ionics* **1983**, *9,10*, 1305.

0897-4756/91/2803-0542$02.50/0

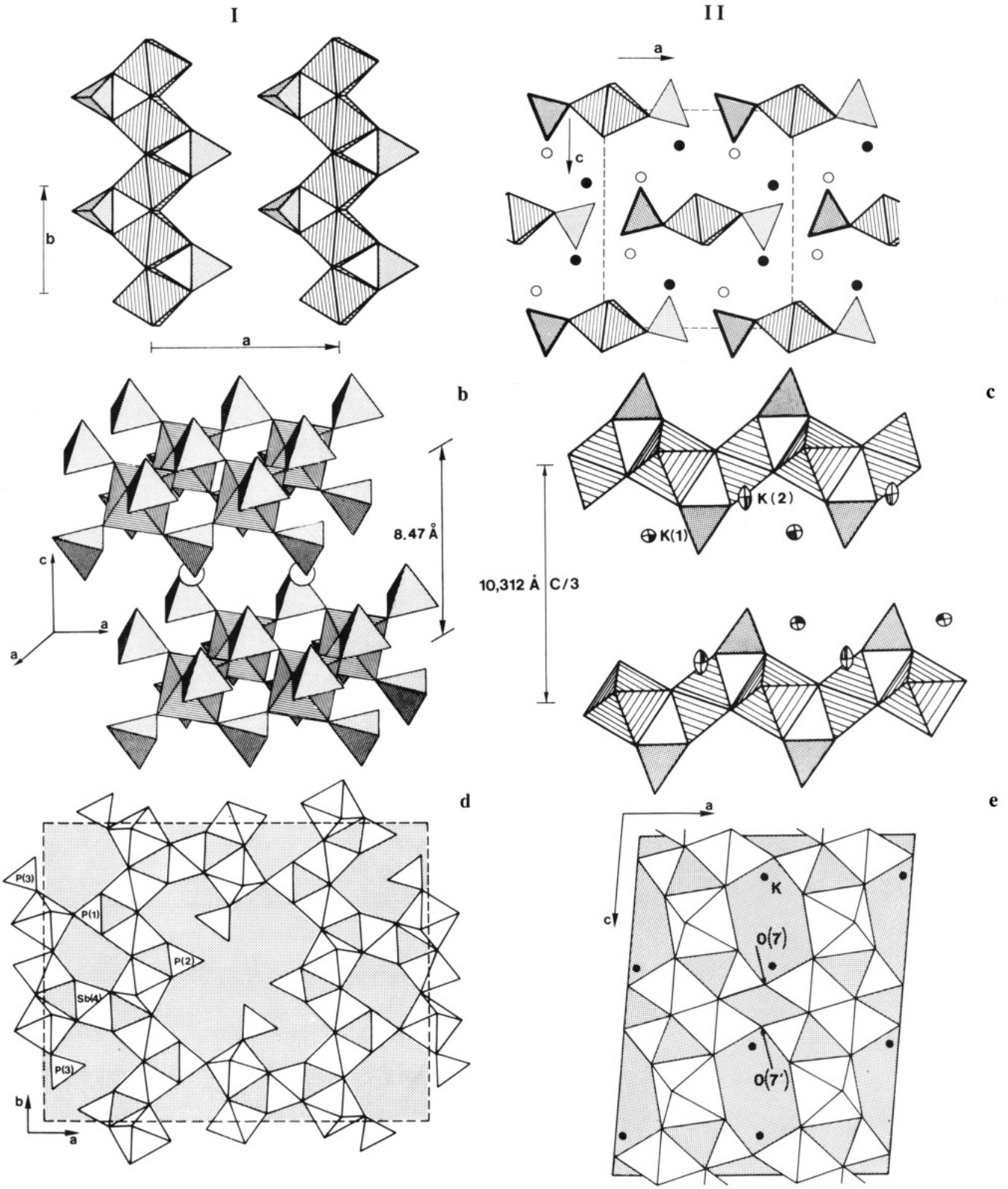

Figure 1. Crystal structure of (a) K_2SbPO_6, (b) $KSbP_2O_8$, (c) $K_3Sb_3P_2O_{14}{\cdot}xH_2O$, (d) $K_5Sb_5P_2O_{20}{\cdot}xH_2O$, and (e) KSb_2PO_8.

the possibility of protonic conduction in addition to K^+ conduction. Thus, to eliminate the protonic conduction, pressed samples were preheated in the conductivity apparatus at 700 °C, and conductivity measurements were carried out in dry flowing helium atmosphere. In addition, a temperature regime was chosen from the TGA curve in which no weight loss was observed. No weight loss was observed at temperatures higher than 250 °C for $K_3Sb_3P_2O_{14}$ and $K_5Sb_5P_2O_{20}$, slight weight loss (~0.5%) was seen in K_2SbPO_6, and no weight loss was observed in $KSbP_2O_8$ and KSb_2PO_8 (Figure 2).

The ionic conductivities for various KPAs are shown in Figure 3. Their conductivities span the range of $\sim 10^{-3}$ to $\sim 10^{-7}$ $(\Omega{\cdot}cm)^{-1}$ from $K_5Sb_5P_2O_{20}$ to KSb_2PO_8 at 500 °C. The conductivity increases gradually from KSb_2PO_8 to $K_3Sb_3P_2O_{14}$; a large increase in conductivity was observed from $K_3Sb_3P_2O_{14}$ to $K_5Sb_5P_2O_{20}$. Correspondingly, the activation energies decrease gradually from 1.02 eV in

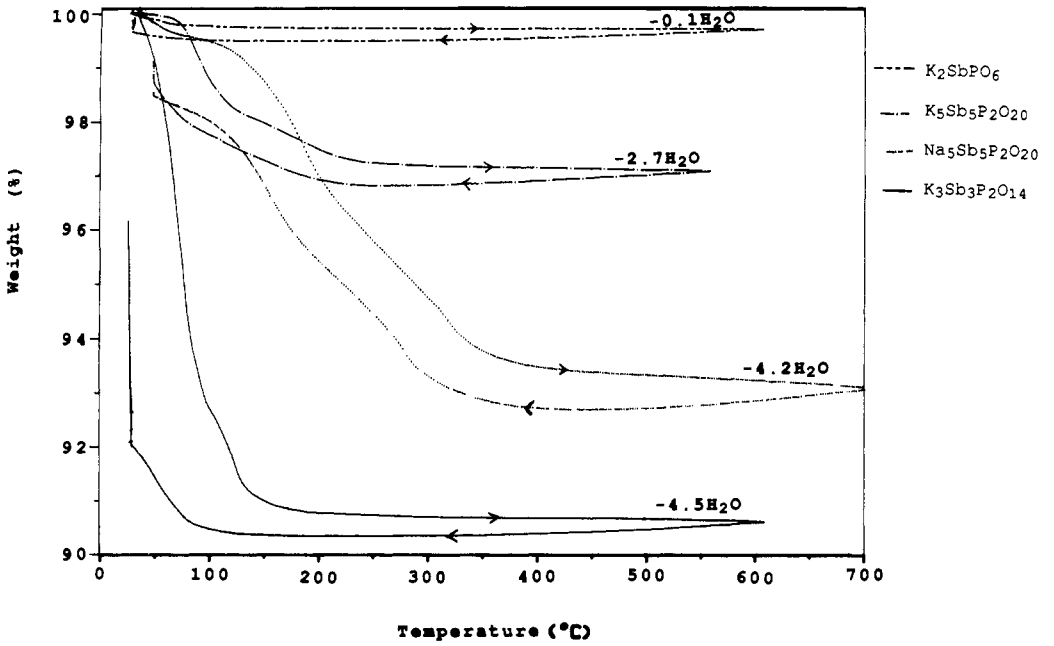

Figure 2. TGA curves of $K_2SbPO_6 \cdot xH_2O$, $K_3Sb_3P_2O_{14} \cdot xH_2O$, $K_5Sb_5P_2O_{20} \cdot xH_2O$, and $Na_5Sb_5P_2O_{20} \cdot xH_2O$.

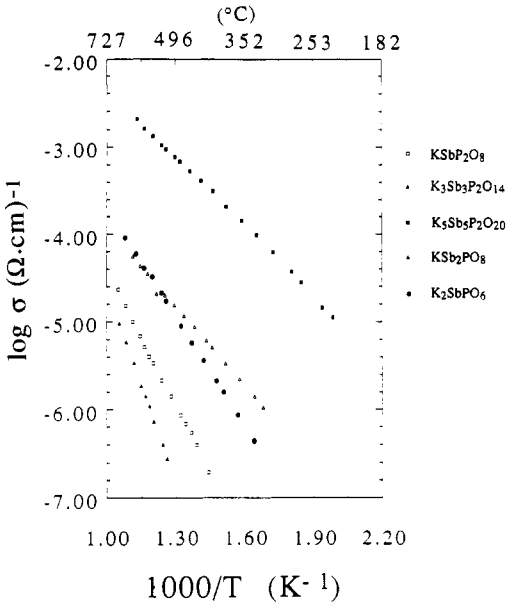

Figure 3. Temperature-dependent ionic conductivities of various potassium phosphatoantimonates.

KSb_2PO_8 to 0.519 eV in $K_5Sb_5P_2O_{20}$. In an attempt to improve the ionic conductivities of the KPAs, ion-exchange reactions were carried out to replace K^+ by other smaller alkali-metal ions.

For $KSbP_2O_8$, $K_3Sb_3P_2O_{14}$, and $K_5Sb_5P_2O_{20}$ ion-exchange reactions with acids already had been reported by Piffard et al.[6,7,13] They also ion exchanged these protonated phosphatoantimonates by Li^+, Na^+, Rb^+, Cs^+, and NH_4^+. However, the chemical stability of the ion-exchanged phosphatoantimonate framework is rather poor, especially

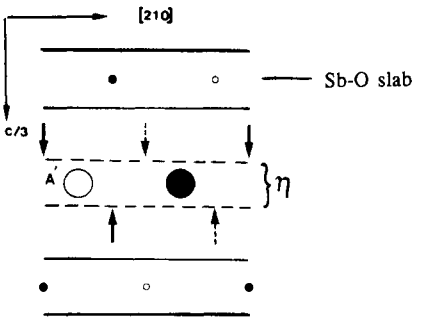

Figure 4. Interlayer distance showing the estimated bottleneck (η) in $KSbP_2O_8$ and $K_3Sb_3P_2O_{14}$ where A' = alkali cation and ↑ represents the unshared terminal P–O bond.

for the highly hydrated samples with small alkali-metal ions. As a result, these ion-exchanged phosphatoantimonates decomposed at a relatively low temperature (about 550 °C) after the loss of hydrated water. Details on the ionic conductivity of alkali-metal phosphatoantimonates ion exchanged from the protonated phosphatoantimonates will be published in a later paper.[13]

Attempts to replace K^+ by Na^+ via ion exchange with NaI in a vacuum-sealed quartz tube resulted in decomposition of the KPAs probably due to the reduction of Sb^{5+}.

The other ion-exchange technique, the molten salt method, was effective in synthesizing $Na_3Sb_3P_2O_{14}$, but $KSbP_2O_8$ and K_2SbPO_6 decomposed upon ion exchange with molten $NaNO_3$. No ion exchange or decomposition was observed for KSb_2PO_8. Finally, the hydrothermal route of ion exchange with aqueous $NaNO_3$ solution in an autoclave was found to be an effective way of synthesizing $Na_5Sb_5P_2O_{20}$.

Discussion

Weight loss observed by TGA for K_2SbPO_6, $K_3Sb_3P_2O_{14}$, and $K_5Sb_5P_2O_{20}$, equilibrated in saturated water vapor at room temperature for 1 day, correspond to 0.1, 4.5, and 2.7 water molecules/molecule of KPA. Surprisingly, no hydration at all was observed in the layered $KSbP_2O_8$, whereas the three-dimensional network structure $K_5Sb_5P_2O_{20}$ is hydrated. This is because the actual interlayer

(9) Deniard-Courant, S.; Piffard, Y.; Barboux, P.; Livage, *J. Solid State Ionics* **1988**, *27*, 189.
(10) Subramanian, M. A.; Subramanian, R.; Clearfield, A. *Solid State Ionics* **1985**, *15*, 15.
(11) Lachgar, A.; Deniard-Courant, S.; Piffard, Y. *J. Solid State Chem.* **1988**, *73*, 572.
(12) Goodenough, J. B.; Hong, H. Y.-P.; Kafalas, J. A. *Mater. Res. Bull.* **1976**, *11*, 203.
(13) Tournoux, M.; Piffard, Y. French Patent 85-10839.

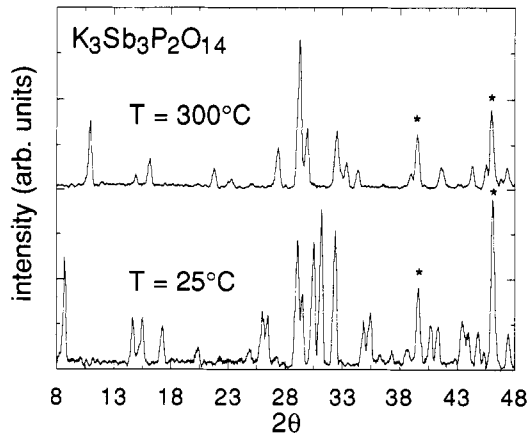

Figure 5. Powder X-ray diffraction at room temperature and 300 °C for $K_3Sb_3P_2O_{14}$. Platinum peaks are indicated by an asterisk.

free space in $KSbP_2O_8$ is about 1.6 Å (~3.5 Å in $K_3Sb_3P_2O_{14}$), (Figure 4), which is too small to accommodate water molecules (minimum interlayer free space ~2 Å). As for $K_5Sb_5P_2O_{20}$, the structure can best be described as a skeleton structure with large interconnected cavities in which ~2.7 water molecules are located. Another example of hydrated skeleton structure can be found in the defect pyrochlore compound, $KTaWO_3 \cdot H_2O$.[10] Finally, in KSb_2PO_8, no hydration was observed at all because the cavities, partially occupied by K^+ in the framework structure, are too small to accommodate water molecules.

Concomitant with the dehydration of $K_3Sb_3P_2O_{14} \cdot 4.5H_2O$, a structural change from rhombohedral to monoclinic symmetry was observed by the high-temperature powder X-ray diffraction (Figure 5), in agreement with Lachgar et al.,[11] who examined the structural details of the phase transition. A similar study was carried out on $K_5Sb_5P_2O_{20}$ and its hydrated phase to elucidate the structure responsible for the observed high ionic conductivity. It was found that both the dehydrated phase above 250 °C and the hydrated phase correspond to the reported structure. However, the hydrated phase has larger unit cell parameters (a = 23.79 Å, b = 18.35 Å, c = 7.130 Å) than those of the dehydrated phase (a = 23.47 Å, b = 18.25 Å, c = 7.109 Å).

We shall now attempt to explain the wide range of ionic conductivity values observed in these KPAs in terms of their structural properties. Several interrelated factors affecting the observed ionic conductivities in these KPA's are (1) dimensionality of the structure, (2) size of the bottleneck for K^+ diffusion, (3) occupancy of available K^+ sites, and (4) strength of the K^+–oxygen bonds.

In K_2SbPO_6, strings of edge-sharing SbO_6 octahedra extend along the b axis, resulting in a quasi-1D structure (Figure 1a). K^+ movement is expected along the a and b directions but somewhat restricted along c because of the obstructing PO_4 groups. The ionic conductivity of K_2SbPO_6 is only $\sim 10^{-5}$ $(\Omega \cdot cm)^{-1}$ at 500 °C (Figure 3). Interestingly, its activation energy (E_a) is higher than that of "2D" $K_3Sb_3P_2O_{14}$ or "3D" $K_5Sb_5P_2O_{20}$ (Table I). This is in agreement with the structural results that the size of the bottleneck for K^+ diffusion in K_2SbPO_6 is smaller than that of $K_3Sb_3P_2O_{14}$ or $K_5Sb_5P_2O_{20}$ (Table I). Another factor for the observed low conductivity could be due to stacking faults, a common defect in quasi-1D compounds, which would lower K^+ conductivity.

Ion exchange of K_2SbPO_6 with alkali-metal ions smaller than K^+ resulted in the collapse of the structure regardless of the ion-exchange methods employed. In contrast,

Table I. Estimated Bottleneck Sizes, Densities, and Activation Energies of Potassium Phosphatoantimonates

compd	interlayer dist or cavity size, Å	est bottle-neck, Å	density,[a] g/cm^3	σ_0	E_a, eV
K_2SbPO_6	9.43	2.47	3.53	2.694	0.821
$KSbP_2O_8$	8.47	1.63	3.501	5.250	1.02
$K_3Sb_3P_2O_{14}$	10.31	3.47	2.798	0.103	0.587
$K_5Sb_5P_2O_{20}$		4.10	3.821	1.909	0.519
KSb_2PO_8		<2.25	4.498	776	1.486

[a] Densities were obtained from refs. 1–5 for K_2SbPO_6, $KSbP_2O_8$, $K_3Sb_3P_2O_{14}$, $K_5Sb_5P_2O_{20}$, and KSb_2PO_8, respectively.

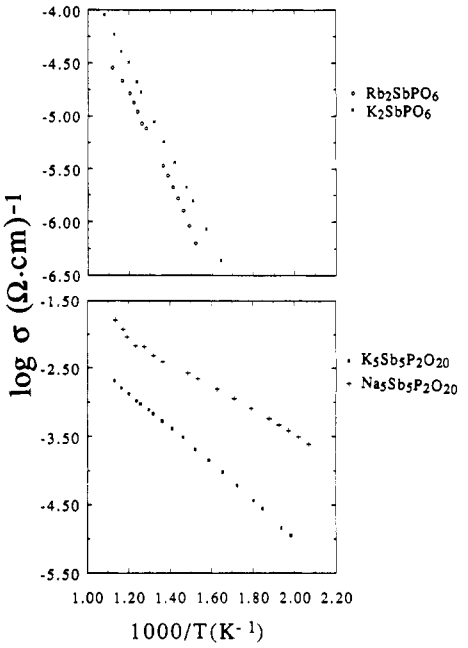

Figure 6. Ionic conductivities of (a, top) Rb_2SbPO_6 and K_2SbPO_6 and (b, bottom) $Na_5Sb_5P_2O_{20}$ and $K_5Sb_5P_2O_{20}$.

complete exchange was observed for ions bigger than K^+ (such as Rb^+), resulting in an increase of unit cell parameters. Thus, the size of the K^+ ion is critical; for smaller ions the separation between the layers (Figure 1aI) is too small, resulting in the collapse of the structure.

Rb_2SbPO_6, prepared for the first time, could be indexed in an orthorhombic symmetry with unit cell constants of a = 9.503 Å, b = 5.950 Å, and c = 11.43 Å. When compared with $K_2Sb_2PO_6$ (a = 9.421 Å, b = 5.889 Å, and c = 11.02 Å), it is evident that the c parameter increases the most, since the cations are located between the chains along the c dimension only (see Figure 1a).

The ionic conductivity of Rb_2SbPO_6 is lower than that of K_2SbPO_6 (Figure 6a) even though their activation energies are about the same. This is because both Rb^+ and K^+ migrate through the same sites (thus the same E_a) but Rb^+ is heavier than K^+ (thus lower ionic mobility).

Both $K_3Sb_3P_2O_{14}$ and $KSbP_2O_8$ exhibit a quasi-2D layered structure, yet the conductivity of $K_3Sb_3P_2O_{14}$ is more than an order of magnitude higher than that in $KSbP_2O_8$ (Figure 3). The difference in conductivity could be attributed to a larger bottleneck in $K_3Sb_3P_2O_{14}$, which has a larger interlayer separation distance than that of $KSbP_2O_8$. The difference in bottleneck size is also evident in the disparity between the potassium thermal factors (Table II) and activation energies of $K_3Sb_3P_2O_{14}$ and $KSbP_2O_8$ (Table I). Moreover, in $K_3Sb_3P_2O_{14}$ there are two equivalent K^+ ions per unit cell and they both contribute to the observed ionic conductivity (the occupancies for both sites

Table II. Potassium Thermal Factors and Occupancies for Potassium Phosphatoantimonates

compd	K^+ sites/position	occupancies	B, Å^3	ref
K_2SbPO_6	K(1)/4c	1	1.80	1
	K(2)/4c	1	1.70	1
$KSbP_2O_8$	K/3b	1	2.16	2
$K_3Sb_3P_2O_{14}\cdot xH_2O$	K(1)/6c	0.883	2.87	3
	K(2)/6c	0.619	4.6	3
$K_5Sb_5P_2O_{20}\cdot xH_2O$	K(6)/8h	0.65	6.0	4
	K(7)/4g	0.48	7.0	4
	K(8)/4g	0.48	7.0	4
	K(9)/4e	0.24	7.0	4
KSb_2PO_8	K(1)/4a	1	2.52	5
	K(1')/4a	1	1.63	5

are less than 1), thus resulting in a higher ionic conductivity than that of $KSbP_2O_8$, which has only one K^+ ion per unit cell.

Attempts were made to improve the ionic conductivities of $K_3Sb_3P_2O_{14}$ and $KSbP_2O_8$ by replacing K^+ with Na^+ via ion-exchange reactions. $Na_3Sb_3P_2O_{14}\cdot 4.2H_2O$ formed by the molten salt method with $NaNO_3$, whereas no exchange was possible with Na^+ in $KSbP_2O_8$. This, coupled with the results of successful ion exchange in $HSbP_2O_8\cdot xH_2O$, shows that the $SbP_2O_8^-$ layers are held too tightly by the K^+ ions in $KSbP_2O_8$. Hence no *direct* ion exchange will be possible in $KSbP_2O_8$. The ionic conductivity of $Na_3Sb_3P_2O_{14}$ indicates some improvement over its K analogue.[14]

The lowest ionic conductivity of all the KPAs studied here was observed in KSb_2PO_8, which has a 3D framework structure with tunnels extending only along the b axis.[5] Even though it shows a potassium thermal factor equivalent to that of "1D" K_2SbPO_6[1] and "2D" $KSbP_2O_8$,[2] it has the highest E_a among the KPAs studied. This is largely due to its highly close packed structure (evidenced by its large density (Table I)), which leads to a small bottleneck for K^+ motion. Another factor for the high E_a in KSb_2PO_8 could be attributed to the lack of vacancies due to the high occupancy factor of K^+ ions (Table II).[14]

Finally, the highest ionic conductivity was observed in $K_5Sb_5P_2O_{20}$, a 3D network structure.[4] This compound also has the smallest E_a and the largest K thermal factor among the KPAs studied. Several factors contribute to the high conductivity observed in $K_5Sb_5P_2O_{20}$. The small E_a is attributed to a large bottleneck (~4.1 Å, calculated by CHEMX) in $K_5Sb_5P_2O_{20}$. Its bottleneck size is comparable with the ~5.3 Å found in the hollandite structure, $K_xM_{x/2}Ti_{8-x/2}O_{16}$ (M = Mg, Zn, Ni), a potassium ion conductor with a conductivity range of 10^{-5}–10^{-3} $(\Omega\cdot cm)^{-1}$ at 200–400 °C.[8] Moreover, there are nine unique K sites per unit cell in $K_5Sb_5P_2O_{20}$, four with low occupancy factors.[4] This leads to the highest mobile K^+ concentration per unit cell among the KPAs studied here. Undoubtedly, the high ionic conductivity also can be attributed to the fact that the K^+ ions are capable of moving in 3D connected tunnels of the skeleton structure. Deniard-Couraut et al. also commented on the remarkably high proton conductivity of $H_5Sb_5P_2O_{20}\cdot xH_2O$.[9]

In many aspects, $K_5Sb_5P_2O_{20}$ exhibits many of the characteristics found in nasicon, $Na_{1+x}Zr_2P_{3-x}Si_xO_{12}$.[11] The nasicon structure is made up of corner-sharing ZrO_6 octahedra and $(P/Si)O_4$ tetrahedra in such a way that three-dimensional intersecting conduction tunnels are formed; an average of three Na^+ per unit cell is found in these tunnels. These similarities prompted us to undertake a study of the ionic conductivity of sodium-exchanged $Na_5Sb_5P_2O_{20}$, in the hope of improving the ionic conductivity of $K_5Sb_5P_2O_{20}$. Interestingly, we found that *direct* ion exchange of Na^+ for K^+ could be achieved only via hydrothermal synthesis with 1 M $NaNO_3$ aqueous solution in an autoclave. Solid-state high-temperature synthesis resulted in a multiphase product, whereas no ion-exchange was observed by the molten salt technique using $NaNO_3$. Thus, water of hydration is needed to stabilize the structure when K^+ is replaced by the smaller Na^+ ions in the tunnel of the structure. Similar results were observed in defect pyrochlores, AB_2X_6[12] (A = alkali-metal ions; B = Nb, Sb, Ta; X = O, F), whereby hydrated compounds were formed with small A^+ ions such as Li^+ or Na^+. Large A^+ ions such as Rb^+ or Cs^+ resulted in dehydrated compounds. TGA measurements indicate that about 4.2 molecules of water are incorporated/molecule of $Na_5Sb_5P_2O_{20}$ as compared to the 1.5 water molecules in $K_5Sb_5P_2O_{20}$, as discussed above. Furthermore, the structure is stable and water loss or uptake is reversible up to 700 °C (Figure 2).

Ionic conductivity measurements carried out in He atmosphere from 200 to 600 °C indicate 1 order of magnitude improvement in the conductivity in the sodium-exchanged $Na_5Sb_5P_2O_{20}$ compared to $K_5Sb_5P_2O_{20}$ (Figure 6b). However, the conductivity at 300 °C is about 2 orders of magnitude lower than that of nasicon, in agreement with the slightly higher activation energy in $Na_5Sb_5P_2O_{20}$ (E_a ~ 0.357 eV) than that of nasicon (E_a ~ 0.25 eV). The difference in E_a and ionic conductivity could be attributed to bottleneck size, strength of the Na^+–lattice oxygen bonds (due to different covalency between the frameworks of $Na_5Sb_5P_2O_{20}$ and nasicon) and available sites for Na^+ diffusion. Work is now in progress to improve the conductivity of $Na_5Sb_5P_2O_{20}$ by aliovalent substitutions.

Conclusions

The original objective of this investigation was to examine the correlation of ionic conductivity with structural dimensionality in a series of KPAs with 1D-to-2D-to-3D structures. All except one, the 3D KSb_2PO_8, showed good ion-exchange properties. On the basis of previous ion-exchange studies,[6,7] the highest ionic conductivity might have been expected in the two-dimensional KPAs. However, this study shows that the ionic conductivity is not correlated well with structural dimensionality. This is consistent with the findings by England, et al.,[15] who showed that a good ion-exchange property is a necessary but not sufficient condition for good ionic conductivity. 3D $K_5Sb_5P_2O_{20}$ has the highest ionic conductivity ($\sigma_{500\,°C}$ ~ 10^{-3} $(\Omega\cdot cm)^{-1}$), and 3D KSb_2PO_8 has the lowest ($\sigma_{500\,°C}$ ~ 10^{-7} $(\Omega\cdot cm)^{-1}$). The ionic conductivity of the 2D phases, $KSbP_2O_8$ and $K_3Sb_3P_2O_{14}$, ranges from ~10^{-4} to 10^{-5} $(\Omega\cdot cm)^{-1}$. Detailed analysis of the Arrhenius plots indicates that the ionic conductivity in KPAs is determined primarily by the "bottleneck" for K^+ diffusion and the concentration of mobile K^+ ions. The preexponential terms (Table I) are different, which is consistent with the differences of the structural properties of the KPAs.

Acknowledgment. We express our gratitude to Prof. Piffard of Universite de Nantes for helpful discussions and providing the structural figures for publication. We also thank Dr. Huan of Exxon for calculating the bottleneck size with the CHEMX. This work was supported by the Office of Naval Research.

(14) Wang, E.; Greenblatt, M., to be published.

(15) England, W. A.; Goodenough, J. B.; Wiseman, P. J. *J. Solid State Chem.* **1983**, *49*, 289.